Venus' Transit 2004: Observations and Analysis of the Black-Drop Effect

Article *in* Romanian Astronomical Journal · January 2007

2 authors:

Adrian Sabin Popescu
Astronomical Institute of Romania

Mircea Rusu
University of Bucharest

VENUS' TRANSIT 2004: OBSERVATIONS AND ANALYSIS OF THE BLACK-DROP EFFECT

ADRIAN SABIN POPESCU[1], MIRCEA RUSU[2]

[1] *Astronomical Institute of the Romanian Academy*
Str. Cuţitul de Argint 5, 040557 Bucharest, Romania
E-mail: sabinp@aira.astro.ro

[2] *University of Bucharest, Faculty of Physics*
Str. Atomiştilor 1, CP MG-11, 077125 Bucharest-Măgurele, Romania
E-mail: mvrusu@yahoo.com

Abstract. The transit of Venus across the solar disk took place on June 8, 2004. Using a fractal method of image processing on TRACE satellite images, we determine the moment (before the third contact) at which the black-drop effect occurred.

Key words: Venus' transit − black-drop effect − image analysis − fractal dimension.

1. INTRODUCTION: FRACTAL ANALYSIS

Everyone knows the dimension of a line, a square, and a cube. They are one, two, and three respectively. And we are able to measure the length, area, and volume of these objects as well. But how do we measure the surface area for kidney, or for the brain, or for broccoli, or for cauliflower? This is where fractal dimension can help us.

The classic example of this is trying to measure a coastline. Actually, it is impossible to precisely measure the length of the coastline. The tide is always coming in or going out, which means that the coastline itself is constantly changing. Therefore, any ordinary measurement is meaningless.

Fractal dimension allows us to measure the degree of complexity by evaluating how fast our measurements increase or decrease as our scale becomes larger or smaller.

We will discuss two types of fractal dimension: self-similarity dimension and box-counting dimension.

There are many different kinds of dimension. Other types include topological dimension, Hausdorff dimension, and Euclidean dimension. It is important to note that not all types of dimension measurement will give the same answer to a single problem. However, our dimension measurements will give the same answer.

The methods we are going to discuss for measuring fractal dimension rely heavily on the power law.

1.1. SELF-SIMILARITY DIMENSION

To measure the self-similar dimension, the picture must be self-similar. The power law holds and in this case is:

$$a = s^{-D},$$

where a is the number of pieces, s is the reduction factor, and D is the self-similar dimension measure.

For instance, if a line is broken into three pieces, each is going to be one-third the length of the original. Therefore $a = 3$, $s = 1/3$, and $D = 1$.

As another example, if a square is broken into four pieces, each side is going to be one-half the original length of the side. Therefore $a = 4$, $s = 1/2$, and $D = 2$.

1.2. BOX-COUNTING DIMENSION

To calculate the box-counting dimension, we need to place the picture on a grid. The x-axis of the grid is s where:

$$s = \frac{1}{\text{width of the grid}}.$$

For instance, if the grid is 240 blocks tall by 120 blocks wide, $s = 1/120$. Then, count the number of blocks that the picture touches. Label this number $N(s)$. Now, resize the grid and repeat the process. Plot the values found on a graph where the x-axis is log (s) and the y-axis is log ($N(s)$). Draw in the line of best fit and find the slope. The box-counting dimension measure is equal to the slope of that line.

The box-counting dimension is much more widely used than the self-similarity dimension since the box-counting dimension can measure pictures that are not self-similar (and most real-life applications are not self-similar).

When we are interested in computing the fractal dimension via box counting, the path to be followed is:

(1) We start with an image which we suspect having a fractal dimension.

(2) We produce a binary version of the image. All pixels above a chosen brightness are set to one, the rest are set to zero.

(3) We produce an image of contours around the bright sections.

(4) We break the image up into boxes of a given size and count how many of those boxes contain the contour. We then repeat this process with several different

box sizes. If a box is white, it contains the contour, if it is black, it does not.

(5) We plot the log of the box size versus the numbers we counted for that box size.

(6) The slope of the resulting plot gives us the fractal dimension of the image.

2. GROUND-BASED VENUS' TRANSIT DETAILS

For the ground-based observations of Venus' transit across the Sun's disk on 8 June 2004, the first contact took place at 05:20:06 UT, the second contact at 05:39:48 UT, the third contact at 11:04:21 UT and the fourth contact at 11:23:40 UT.

3. BLACK-DROP STUDY

We are interested in determining the moment at which the black drop begins to manifest itself, before the third contact.

The fractal-dimension change implies a modification of the conditions in the development of a process. For a constant process at equilibrium we have a constant fractal dimension. When the process conditions are varying as function of constant parameters, also the fractal dimension will have an evolution without inflexion points. But, when in a process a new process appears, this produces inflexion points and all this can be seen only by the variation of the black and white pixels contained in an area of the analyzed image.

Our studies were done on images taken by the TRACE satellite, processed with the code "Fractal Analysis", developed by V. Grosu, C. Beşliu and M. Rusu.

The advantage presented by the satellite images is the lack of atmospheric turbulence, which is a major factor of perturbation for observation and a supplementary process to be eliminated in order to obtain the black-drop effect.

The available TRACE images under study have the resolution of 512×512 and 1024×512 pixels.

In white light, on the solar surface, the limb darkening affects the fractal dimension. Far from the solar edge the fractal dimension is unaffected by the limb darkening (Figs. 1, 2), while in the proximity of the solar limb it is strongly affected by it (Figs. 3, 4). On larger scales, in white light, the fractal dimension is affected also by the solar granulation. Because of this, we computed the fractal dimension for a larger area centered on Venus (Fig. 5). The obtained D as function of UT is represented, for the two TRACE image resolutions, in Figs. 6, 8 and 10 (the lower curves).

The first point of inflexion, where the fractal dimension is changing from a constant value to a monotonically increasing function, is due to the limb darkening effect. The second point of inflexion represents the point at which the black-drop effect

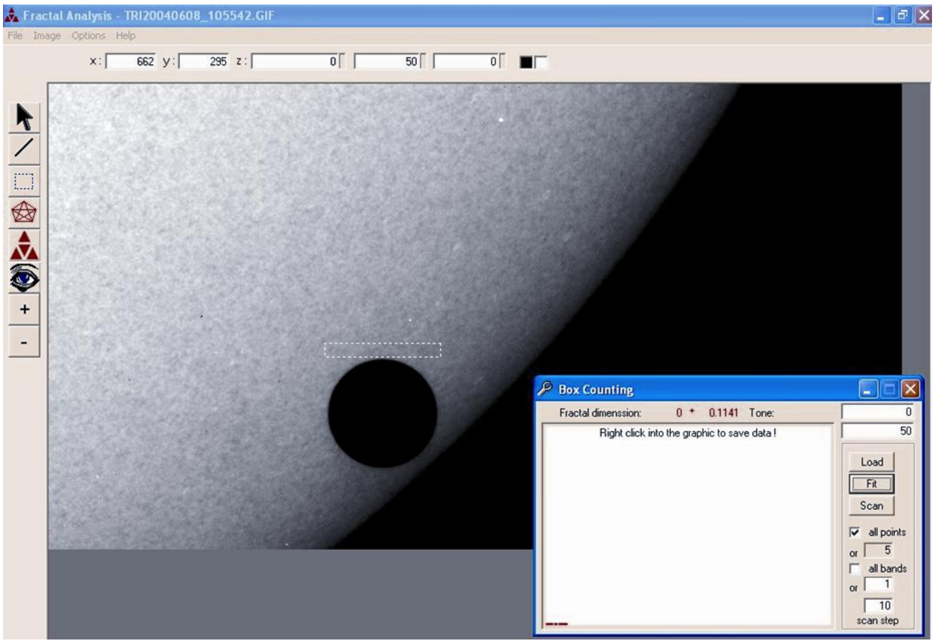

begins to manifest itself.

Fig. 1 – Screen capture with “Fractal Analysis” applied on the image taken at 10:55:42 UT. The fractal dimension on the solar surface, far from the solar limb, is zero (no limb darkening).

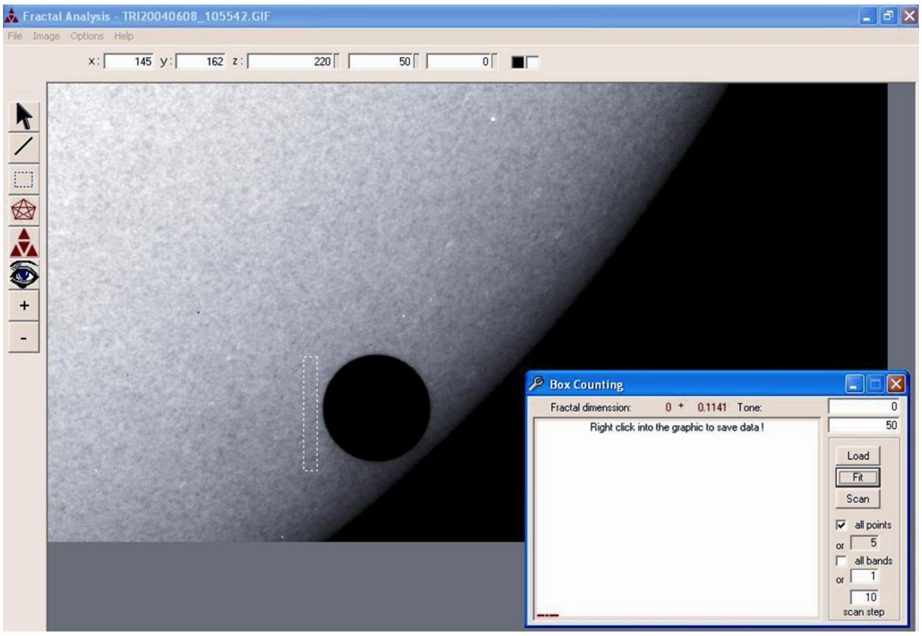

Fig. 2 – Screen capture with "Fractal Analysis" applied on the image taken at 10:55:42 UT. The

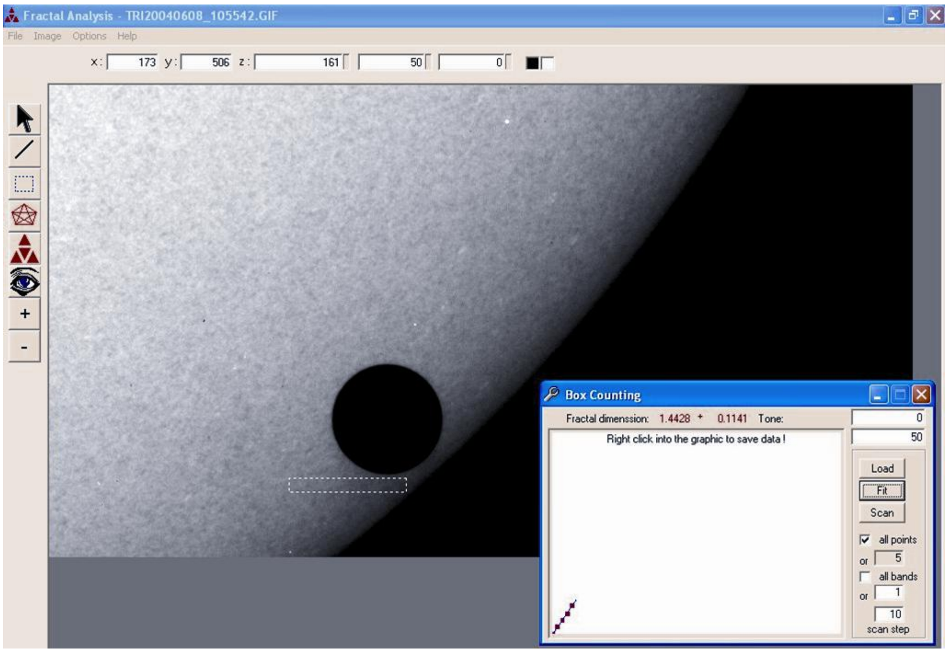

fractal dimension on the solar surface, far from the solar limb, is zero (no limb darkening).

Fig. 3 – Screen capture with "Fractal Analysis" applied on the image taken at 10:55:42 UT. The fractal dimension on the solar surface, close to the solar limb, is ≈ 1.44 (limb darkening).

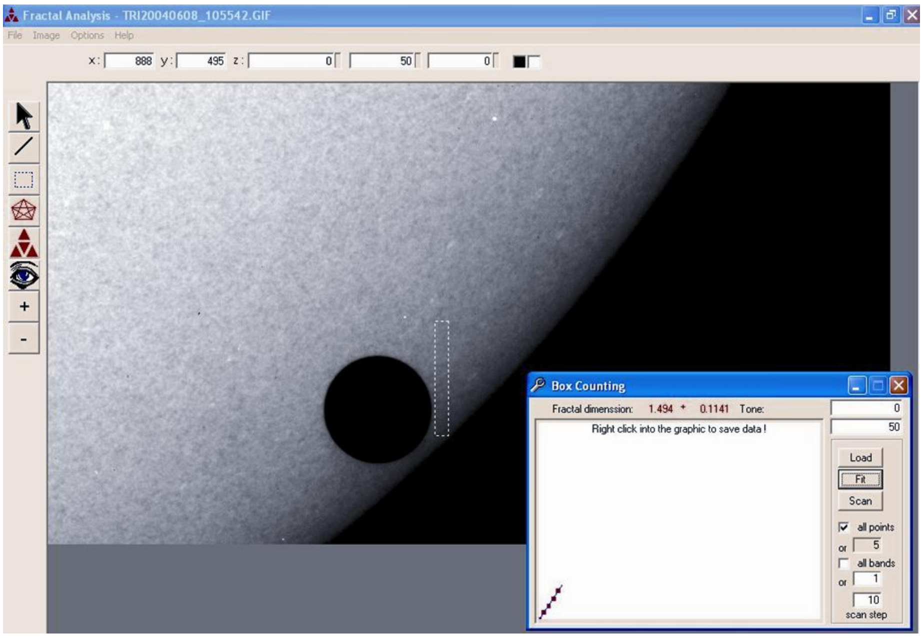

Fig. 4 − Screen capture with the code “Fractal Analysis” applied on the image taken at 10:55:42 UT. The fractal dimension on the solar surface, close to the solar limb, is ≈ 1.49 (limb darkening).

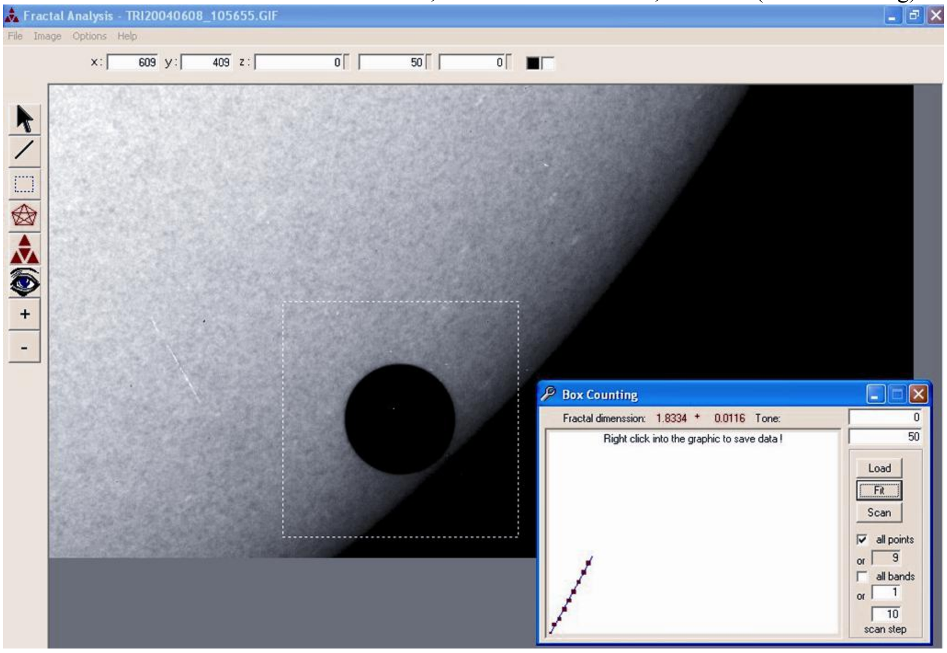

Fig. 5 − Screen capture with “Fractal Analysis” applied on the image taken at 10:56:55 UT. Here we analyze a 1024×512 image for “Venus & Sun” granulation and limb darkening combined effects.

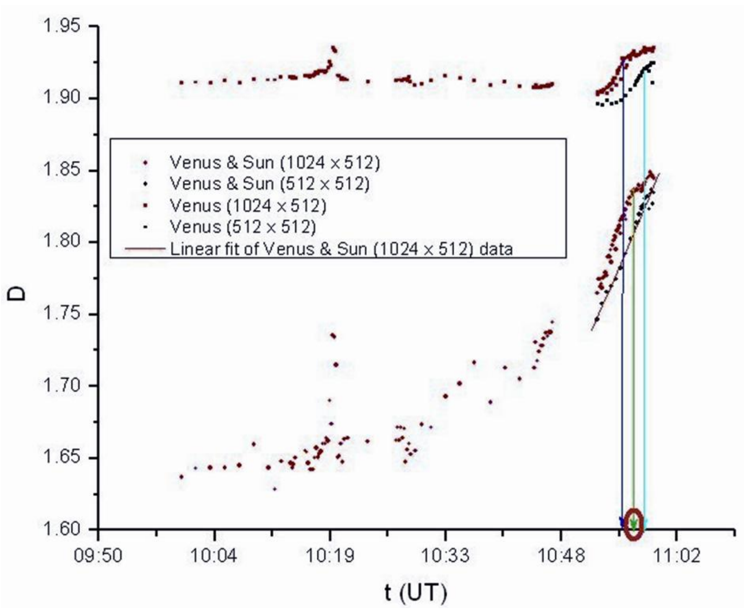

Fig. 6 – Graphical representation of the fractal dimension variation with UT. The identified moment

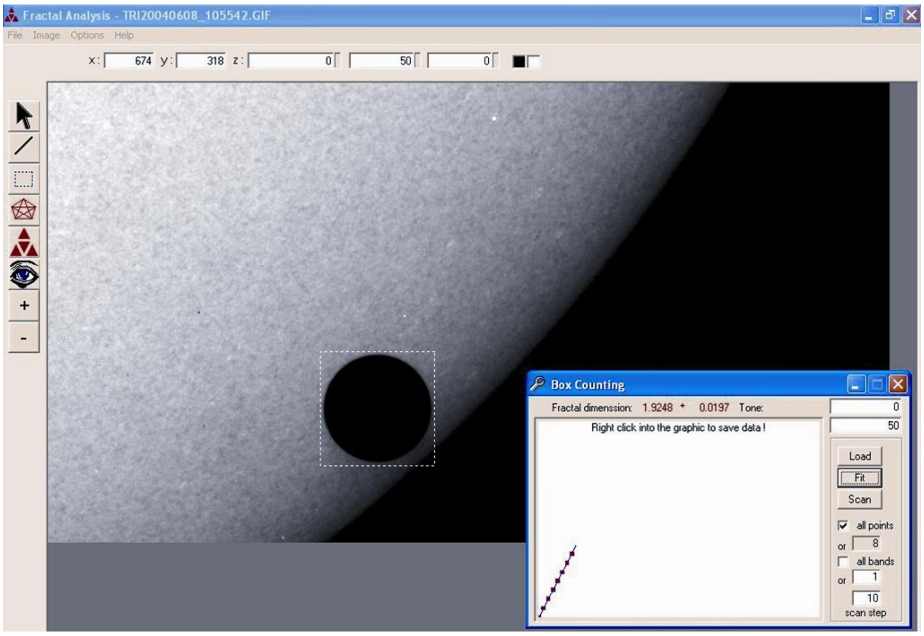

at which the black-drop effect begins to affect the images is 10:56:53 UT.

Fig. 7 – Screen capture with "Fractal Analysis" applied on the image taken at 10:55:42 UT. Here we analyze a 1024×512 image for Venus limb darkening effect.

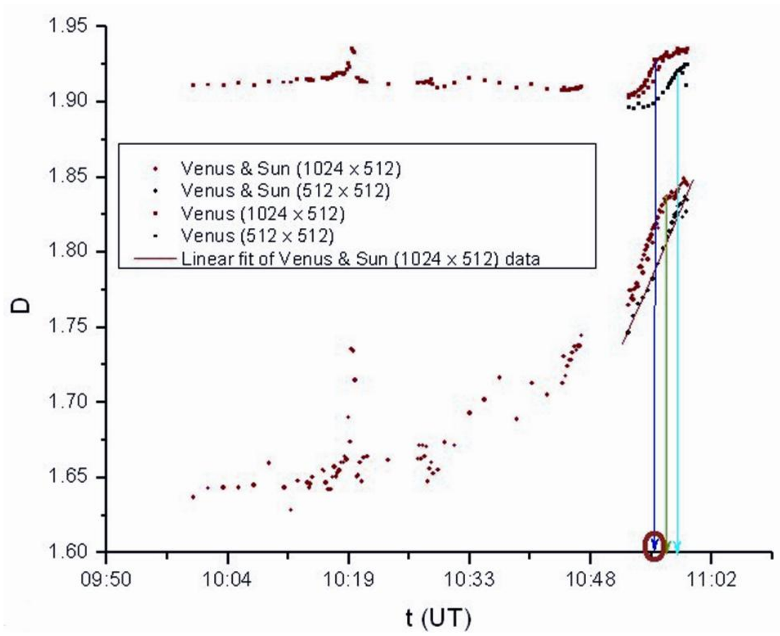

Fig. 8 – Graphical representation of the fractal dimension variation with UT. The identified moment

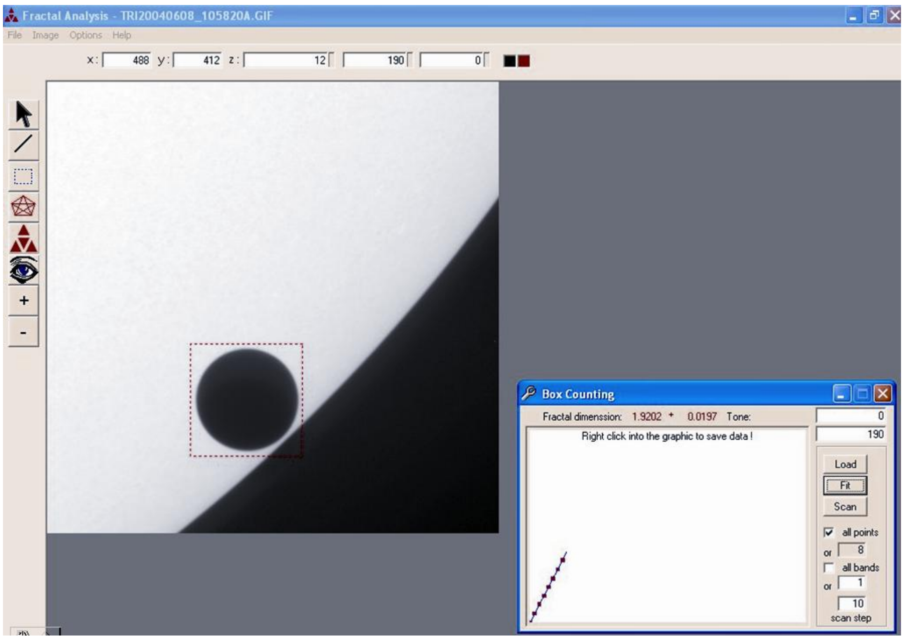

at which the black-drop effect begins to affect the 1024×512 images is 10:55:40 UT.

Fig. 9 − Screen capture with "Fractal Analysis" applied on the image taken at 10:58:20 UT. Here we analyze a 512×512 image for Venus limb darkening effect.

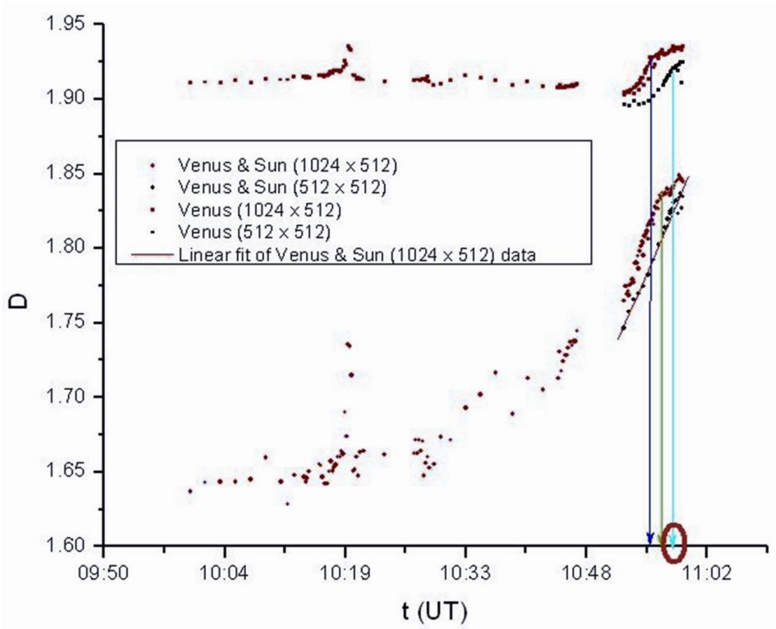

Fig. 10 – Graphical representation of the fractal dimension variation with UT. The identified moment

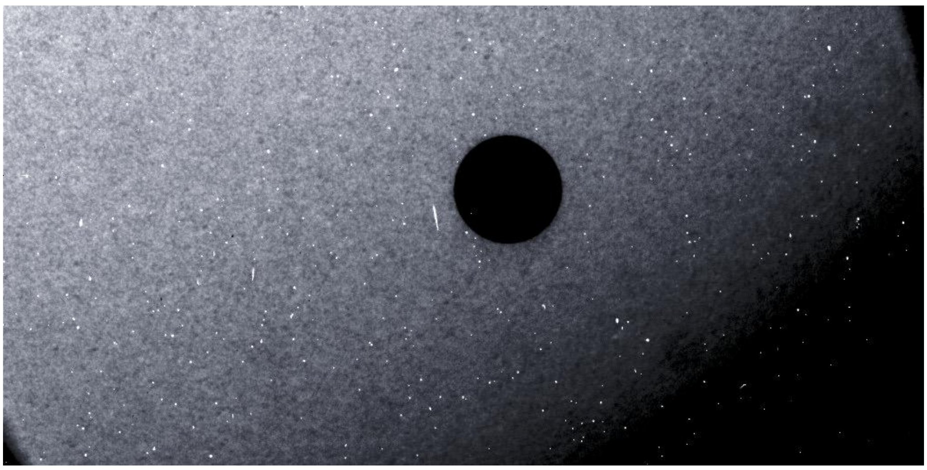

at which the black-drop effect begins to affect the 512×512 images is 10:58:17 UT.

Fig.11 – An example of bad TRACE image affecting our results at $t \approx$ 10:19 UT.

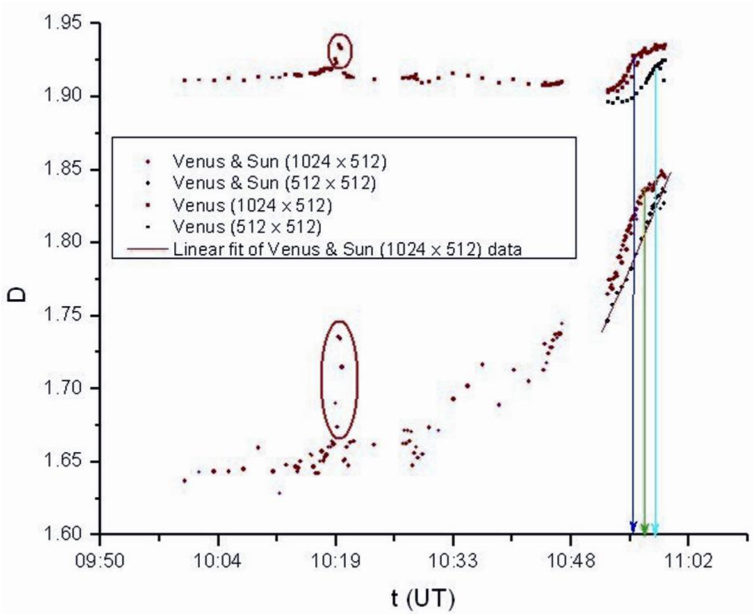

Fig. 12 – Bad data points at $t \approx$ 10:19 UT.

On the 1024×512 and the 512×512 resolution images we were able to determine that the second inflexion point appears at 10:56:53 UT (Fig. 6).

For a box containing Venus and a small area of solar surface (Figs. 7 and 9), unaffected by granulation (the area is smaller than the area of the Fig. 1 and Fig. 2 boxes), we determined that the black-drop effect appears at 10:55:40 UT for the 1024×512 images (Fig. 8) and, for the 512×512 images, at 10:58:17 UT (Fig. 10).

The reason for the hump at approximately 10:19 UT (Fig. 12) in the graph is the bad quality of the TRACE images (Fig. 11).

4. CONCLUSIONS

By using the TRACE satellite observations. we eliminated the effects that “pollute” the fractal dimension behavior of the ground-based observations (atmospheric turbulence, clouds), making possible a more accurate determination of the moment at which the black-drop effect occurs. However, because of the difference of position between the Earth and the satellite relative at the moment of Venus’ transit, we cannot account for a coincidence between the moments at which the black drop occurs in the two locations. Also, eliminating the atmosphere (turbulence) makes the solar edge sharper and, consequently, a later occurrence of the studied effect for TRACE relative to Earth observations.

From the second change of trend into the $D = f(t)$ plots we conclude that the only remaining effects that can produce the black-drop effect are instrument related: image resolution and point spread function.

The resolution dependence of the black-drop occurrence time is as follows:

− 10:56:53 UT for “Venus and Sun” fractal dimension study on 1024×512 images and 512×512 images;

− 10:55:40 UT for “Venus” fractal dimension study on 1024×512 images;

− 10:58:17 UT for “Venus” fractal dimension study on 512×512 images.

The better quality of the 1024×512 images determines us to conclude that, for the TRACE images (at its location), the black-drop effect begins at 10:55:40 UT.

Ground-based observations determined that the black drop appeared at around 11:04 UT, while in the TRACE images it is clear that at 10:59:15 UT the fourth contact already passed.

Received on 20 December 2006